

Josephson current through a Kondo molecule

Rosa López

Departament de Física, Universitat de les Illes Balears, E-07122 Palma de Mallorca, Spain

Mahn-Soo Choi

*Department of Physics, Korea University, Seoul 136-701, Korea
and Department of Physics and Astronomy, University of Basel, Klingelbergstrasse 82, 4056 Basel, Switzerland*

Ramón Aguado

Teoría de la Materia Condensada, Instituto de Ciencia de Materiales de Madrid (CSIC) Cantoblanco, 28049 Madrid, Spain

(Received 20 September 2006; published 30 January 2007)

We investigate transport of Cooper pairs through a double quantum dot in the Kondo regime and coupled to superconducting leads. Within the nonperturbative slave boson mean-field theory we evaluate the Josephson current for two different configurations, the double quantum dot coupled *in parallel* and *in series* to the leads. We find striking differences between these configurations in the supercurrent versus the ratio t/Γ , where t is the interdot coupling and Γ is the coupling to the leads: the critical current I_c decreases monotonously with t/Γ for the parallel configuration whereas I_c exhibits a maximum at $t/\Gamma=1$ in the serial case. These results demonstrate that a variation of the ratio t/Γ enables one to control the flow of supercurrent through the Kondo resonance of the double quantum dot.

DOI: [10.1103/PhysRevB.75.045132](https://doi.org/10.1103/PhysRevB.75.045132)

PACS number(s): 72.15.Qm, 73.23.-b, 74.45.+c

I. INTRODUCTION

The Kondo effect arises whenever a localized spin couples antiferromagnetically with itinerant electrons. At temperatures $T \ll T_K$, where T_K is the Kondo temperature, the spin of the impurity is screened entirely by the conduction electrons, leading to enhanced scattering at the Fermi surface.¹ This new scattering channel (which is reflected in the density of states of the impurity electron at the impurity site as a new quasiparticle resonance of width T_K , the Abrikosov-Shul or Kondo resonance) changes completely the low temperature properties of the system. In the context of mesoscopic physics, a poorly transmitting quantum dot in the Coulomb blockade regime, $T \gg T_K$, becomes perfectly conducting (unitary limit) as the temperature decreases well below T_K .² The experimental demonstration of this effect³ is one of the most spectacular examples of the unprecedented control over artificial Kondo impurities⁴ that nanotechnology offers. This, together with the possibility of studying new aspects of Kondo physics, has renewed interest in this problem.⁵

One of these aspects concerns the study of the competition between superconductivity and Kondo effect⁶ in a controlled manner. This can be realized by coupling a quantum dot to superconducting electrodes. The subgap transport through the Andreev bound states^{7,8} in such a nanostructure is strongly affected by Kondo physics, leading to the phase transition in the sign of Josephson current.⁹ The large Coulomb interaction prevents the tunneling of Cooper pairs into the quantum dot; electrons in each pair tunnel one by one via virtual processes.¹⁰ Due to Fermi statistics, this results in a negative supercurrent (i.e., a π -junction). However, this argument is only valid in the weak coupling limit, when the gap Δ is larger than T_K . In the opposite strong coupling limit ($\Delta/T_K \ll 1$) the Kondo resonance restores the positive Josephson current.^{9,11} This effect has been confirmed experi-

mentally in a superconductor-dot-superconductor system.⁶

A natural step forward is to study a double quantum dot coupled to superconductors. Choi, Bruder, and Loss¹² studied the spin-dependent Josephson current through a double quantum dot in the Coulomb blockade regime. Here, we study a double quantum dot in the Kondo regime (Kondo molecule), *both* in parallel and in series configurations at zero temperature. Both configurations show striking differences in the supercurrent as a function of the ratio t/Γ , where t is the interdot coupling and Γ is the coupling to the leads: the critical current I_c decreases monotonously with t/Γ for the parallel configuration whereas I_c exhibits a maximum at $t/\Gamma=1$ in the serial case.

II. MODEL

The system is modeled as a two-impurity Anderson Hamiltonian where the normal metallic leads are replaced by standard BCS s -wave superconductors:

$$\begin{aligned} \mathcal{H} = & \sum_{k\alpha \in \{L,R\}\sigma} \xi_{k\alpha} c_{k\alpha\sigma}^\dagger c_{k\alpha\sigma} + \sum_{k\alpha} \{ \Delta_\alpha \exp^{i\phi_\alpha} c_{k\alpha\uparrow} c_{-k\alpha\downarrow} + \text{H.c.} \} \\ & + \sum_{i \in \{1,2\}\sigma} (\epsilon_{i\sigma} n_{i\sigma} + U_i n_{i\sigma} n_{i\bar{\sigma}}) + U_{12} n_1 n_2 \\ & + t \sum_{\sigma} \{ d_{1\sigma}^\dagger d_{2\sigma} + \text{H.c.} \} + \sum_{i,k,\alpha,\sigma} \{ V_{i,k\alpha} c_{k\alpha\sigma}^\dagger d_{i\sigma} + \text{H.c.} \}. \quad (1) \end{aligned}$$

$c_{k\alpha\sigma}$ ($d_{i\sigma}$) describes the electrons with momentum k and spin σ in the lead α (the dot i); $n_{i\sigma} \equiv d_{i\sigma}^\dagger d_{i\sigma}$ is the occupation per spin σ for the dot i . ϕ_α and Δ_α denote the superconducting phase and the superconducting gap, respectively, for the lead α . The tunneling amplitude between the dots is given by t and $V_{i,k\alpha}$ corresponds to the tunneling amplitude between the dots and leads. For a double quantum dot in a series

$$V_{1,kR} = V_{2,kL} = 0, \quad V_{1,kL} = V_{2,kR} = V_0, \quad (2)$$

and for a double quantum dot in parallel

$$V_{1,kR} = V_{1,kL} = V_{2,kL} = V_{2,kR} = V_0. \quad (3)$$

ε_i are the single-particle energies on the dots tuned by gate voltages. U_i is the on-site Coulomb interaction on the i th dot, and U_{12} is the interdot Coulomb interaction.

We are interested in the limit $U_1, U_2 \rightarrow \infty, U_{12} = 0$, and $-\varepsilon_i \gg \Gamma$ at zero temperature so that $\langle n_1 \rangle = \langle n_2 \rangle = 1$. The model in this limit is well-described in the slave-boson language.¹³ In this limit, the model can be written in a slave-boson language by applying the transformation $d_{i,\sigma} = b_i^\dagger f_{i,\sigma}$. Here, $f_{i,\sigma}$ is a pseudofermion which destroys one occupied state on quantum dot i and b_i^\dagger is a boson which creates one empty state on quantum dot i .¹³ We then introduce two constraints which prevent double occupancy in each dot by means of Lagrange multipliers, λ_1 and λ_2 .^{1,13} The resulting model is solved within the mean-field approach, namely, replacing $b_i(t) \rightarrow \langle b_i \rangle \equiv \sqrt{N} \tilde{b}_i$, where N is the degeneracy of the impurity level. This so-called slave-boson mean field theory (SBMF) is only valid for describing the deep Kondo limit (spin fluctuations). Charge fluctuations can be included to lowest order as $1/N$ corrections.¹ This approach has been applied successfully to Kondo double quantum dots coupled to normal metallic leads.¹⁴

$$\begin{aligned} \mathcal{H}_{\text{SBMF}} = & \sum_{k\alpha \in \{L,R\}\sigma} \xi_{k\alpha} c_{k\alpha\sigma}^\dagger c_{k\alpha\sigma} \\ & + \sum_{k\alpha} \{ \Delta_\alpha \exp^{i\phi_\alpha} c_{k\alpha\uparrow} c_{-k\alpha\downarrow} + \text{H.c.} \} \\ & + \sum_{i \in \{1,2\}\sigma} \tilde{\varepsilon}_{i\sigma} n_{i\sigma} + \tilde{t} \sum_{\sigma} \{ f_{1\sigma}^\dagger f_{2\sigma} + \text{H.c.} \} \\ & + \sum_{i,k,\alpha,\sigma} \{ \tilde{V}_{i,k\alpha} c_{k\alpha\sigma}^\dagger f_{i\sigma} + \text{H.c.} \} + \lambda_i (N \tilde{b}_i^2 - 1). \quad (4) \end{aligned}$$

The SBFM version of \mathcal{H} [see Eq. (4)] is now quadratic and contains four parameters, i.e., $\tilde{b}_{1,2}$ that renormalize the tunneling amplitudes, $\tilde{V}_{i,k\alpha} = \tilde{b}_i V_{i,k\alpha}$ and $\tilde{t} = t \tilde{b}_1 \tilde{b}_2$, and $\lambda_{1(2)}$ that renormalizes the energy levels $\tilde{\varepsilon}_{1,2\sigma} = \varepsilon_i + \lambda_{1,2}$. They are determined from the solution of the SBFM equations in a self-consistent fashion.

The SBFM equations become simpler in the *Nambu-Keldysh* space where

$$\Psi_{k\alpha\sigma}^\dagger = (c_{k\alpha\sigma}^\dagger c_{-k\alpha\bar{\sigma}}), \quad \Phi_{i\sigma}^\dagger = (f_{i\sigma}^\dagger f_{i\bar{\sigma}}) \quad (5)$$

are the spinors for the conduction and localized electrons. These mean-field equations are obtained from the equation-of-motion of the boson fields and the constrains:

$$\tilde{b}_{1(2)}^2 + \frac{1}{N} \sum_{\sigma} \langle \Phi_{1(2)\sigma}^\dagger(t) \hat{\sigma}_z \Phi_{1(2)\sigma}(t) \rangle = \frac{1}{N}, \quad (6a)$$

$$\begin{aligned} & \frac{1}{N} \sum_{\alpha \in \{L,R\}\sigma} \tilde{V}_{1(2),k\alpha} \langle \Psi_{k\alpha\sigma}^\dagger(t) \hat{\sigma}_z \Phi_{1(2)\sigma}(t) \rangle \\ & + \frac{\tilde{t}}{N} \sum_{\sigma} \langle \Phi_{1(2)\sigma}(t) \hat{\sigma}_z \Phi_{2(1)\sigma}(t) \rangle + \lambda_{1(2)} \tilde{b}_{1(2)}^2 = 0. \quad (6b) \end{aligned}$$

This system of mean-field equation can be written in terms of the 2×2 matrix lesser Green function for the dots $[G_{i,j\sigma}(t,t')]$ and the lead-dot matrix lesser Green function $[G_{i,k\alpha\sigma}(t,t')]$, respectively

$$\begin{aligned} \hat{G}_{i,j\sigma}(t,t') &= i \langle \Phi_{j\sigma}^\dagger(t'), \Phi_{i\sigma}(t) \rangle, \\ \hat{G}_{i,k\alpha\sigma}(t,t') &= i \langle \Psi_{k\alpha\sigma}^\dagger(t'), \Phi_{i\sigma}(t) \rangle. \quad (7) \end{aligned}$$

As usual, the diagonal components of the matrix, G and \tilde{G} , correspond to “electronlike” and “holelike” Green functions whereas off-diagonal components, F and F^\dagger , correspond to anomalous Green functions.

Following the standard procedure, the lesser Green functions are obtained applying rules of analytical continuation along a complex time contour to the equation of motion of the time-ordered Green function (for details, see Refs. 15 and 16). The two off-diagonal Green functions, namely, $\hat{G}_{i,j\sigma}$ (with $i \neq j$) lead-dot Green function $\hat{G}_{i,k\alpha\sigma}$ can be cast in terms of the diagonal dot Green function $\hat{G}_{i,i\sigma} \equiv \hat{G}_{i\sigma}$ using the equation of motion technique. Hereforth, for simplicity we assume a symmetric structure with $\varepsilon_{1(2)\sigma} = \varepsilon_{0\sigma}$, $\Delta_{L(R)} = \Delta$, and $\phi_L = -\phi_R = \phi$. Then, the system of SBFM equations in terms of the dots Green function becomes (for simplicity we omit the spin indices)

$$\frac{\tilde{\Gamma}}{\Gamma} + \int_{-\infty}^{\infty} \frac{d\epsilon}{2\pi i} [G_{1(2)}^<(\epsilon) + \tilde{G}_{1(2)}^<(\epsilon)] = 0, \quad (8a)$$

$$\begin{aligned} \frac{\tilde{\Gamma}}{\Gamma} (\tilde{\varepsilon}_{1(2)} - \varepsilon_{1(2)}) + \int_{-\infty}^{\infty} \frac{d\epsilon}{2\pi i} [G_{1(2)}^<(\epsilon) (\epsilon - \tilde{\varepsilon}_{1(2)}) \\ + \tilde{G}_{1(2)}^<(\epsilon) (\epsilon + \tilde{\varepsilon}_{1(2)})] = 0, \quad (8b) \end{aligned}$$

where $\tilde{\varepsilon}_i = \varepsilon_0 + \lambda_i$ are the renormalized levels and $\tilde{\Gamma}_i = \tilde{b}_i^2 \Gamma$ the renormalized hybridization, which are equal to the Kondo temperature T_K for the coupled system¹⁷ [$\tilde{\Gamma} = 2\pi\rho_N V_0^2$ with ρ_N being the normal-state density of states].

At equilibrium we can employ $\hat{G}_i^< = 2if(\epsilon)\text{Im} \hat{G}_i^r$ with $f(\epsilon)$ being the Fermi function. \hat{G}_i^r is determined by the lead-dot $\hat{\Sigma}_{i\alpha}^r$ and the interdot tunneling $\hat{\Sigma}_{ii}^r$ self-energies. Thus the matrix elements of the lead-dot self-energy are

$$\hat{\Sigma}_{i\alpha}^r = -i\tilde{\Gamma}_i \begin{pmatrix} 1 & \Delta \exp(i\phi_\alpha)/|\epsilon| \\ \Delta \exp(-i\phi_\alpha)/|\epsilon| & 1 \end{pmatrix}, \quad (9)$$

with

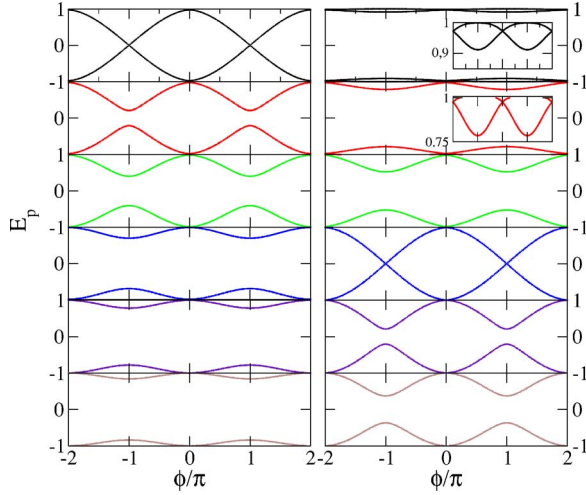


FIG. 1. (Color online) Andreev bound states in units of Δ . Left panel: Parallel case for $t/\Gamma=0, 0.25, 0.5, 1, 1.25$, and 1.5 (from top to bottom). Right panel: Serial case for $t/\Gamma=0.1, 0.25, 0.5, 1, 1.25$, and 1.5 (from top to bottom). In both cases $\Delta=0.17T_K^0$.

$$\rho_S(\epsilon) = \frac{|\epsilon|}{\sqrt{\epsilon^2 - \Delta^2} \theta(\epsilon - \Delta)}, \quad (10)$$

as the superconducting density of states. The interdot tunneling self-energy is

$$\hat{\Sigma}_{i1(2)}^r = \tilde{t}^2 \hat{\sigma}_z \left[g_{2(1)}^r - \sum_{\alpha} \hat{\Sigma}_{2(1)\alpha}^r \right] \hat{\sigma}_z, \quad (11)$$

where σ_z is the z component of the Pauli matrices and \hat{g}_i^r is the matrix Green function for an isolated quantum dot. Since we deal with a symmetric structure $\lambda_i = \lambda \rightarrow \tilde{\epsilon}_i = \tilde{\epsilon}_0$ and $\tilde{\Gamma} = \tilde{\Gamma}_i$. Thus, for example, the diagonal components of the dot Green function for the serial configuration read

$$G^{r(a)} = \frac{(A \pm \tilde{\epsilon}_0)[(A^2 - \tilde{\epsilon}_0^2) - s(\epsilon)^2 + \tilde{t}^2(A \mp \tilde{\epsilon}_0)]}{\mathcal{D}(\epsilon)}, \quad (12)$$

where

$$\mathcal{D}(\epsilon) = [A^2 - X^2 - Y^2 - (\tilde{\epsilon}_0 - \tilde{t})^2]^2 - 4\tilde{t}^2(Y^2 + \tilde{\epsilon}_0^2),$$

with

$$X = s(\epsilon)\cos(\phi), \quad Y = s(\epsilon)\sin(\phi),$$

$$A = \epsilon[1 + s(\epsilon)/\Delta], \quad s(\epsilon) = \Delta\tilde{\Gamma}/\sqrt{\Delta^2 - \epsilon^2}. \quad (13)$$

The Green function (12) describes the discrete Andreev bound states in the subgap region ($|\epsilon| < \Delta$) as well as the continuum spectrum above the gap ($|\epsilon| > \Delta$). The Andreev states appear as poles of the Green function; i.e., the solutions of $\mathcal{D}(\epsilon)=0$ (see Fig. 1). Accordingly, the Josephson current has two contributions,

$$I_{\text{tot}} = I_{\text{dis}} + I_{\text{con}}, \quad (14)$$

where I_{dis} is from the discrete Andreev states and I_{con} from the continuum (see Figs. 2 and 3). I_{tot} can be obtained from

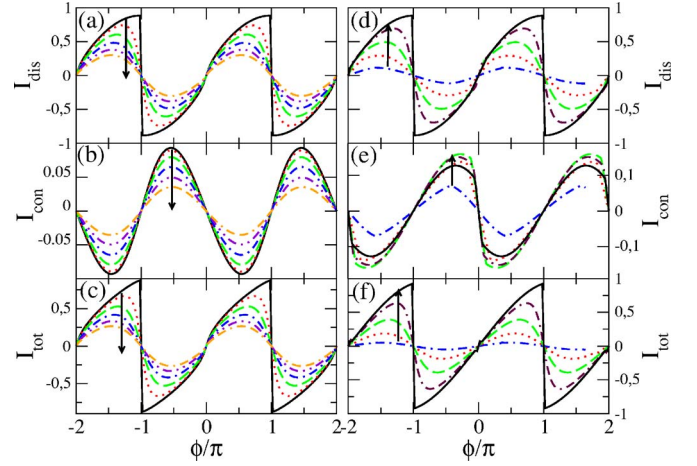


FIG. 2. (Color online) $t/\Gamma \leq 1$. Left (right) panel corresponds to the parallel (serial) case. (a) and (d) discrete I_{dis} , (b) and (e) continuum I_{con} , and (c) and (f) total supercurrent I_{tot} vs ϕ for $t/\Gamma=0, 0.2, 0.4, 0.6, 0.8$, and 1 ($t/\Gamma=0.2, 0.4, 0.6, 0.8$, and 1) and $\Delta=0.17T_K^0$. Currents are in units of $2|e|/\Delta\hbar$. The curves are arranged with increasing t/Γ in the direction of the arrows.

the evolution of the quantum particle operator of the left contact

$$I_{\text{tot}} = -ie\langle \dot{N}_L \rangle, \quad N_L = \sum_{kL,\sigma} c_{kL\sigma}^\dagger c_{kL\sigma}. \quad (15)$$

The total current, for instance, for the serial case, is given by

$$I_{\text{tot}} = \frac{2e}{\hbar} \text{Re} \sum_{kL\sigma} \tilde{V}_0 \left\{ \int dt [G_{1,kL\sigma}^<(t,t) - \tilde{G}_{1,kL\sigma}^<(t,t)] \right\}, \quad (16)$$

where $\tilde{V}_0 = \tilde{b}V_0$. Thus the two parts of the Josephson current for the double quantum dot in series at zero temperature (see

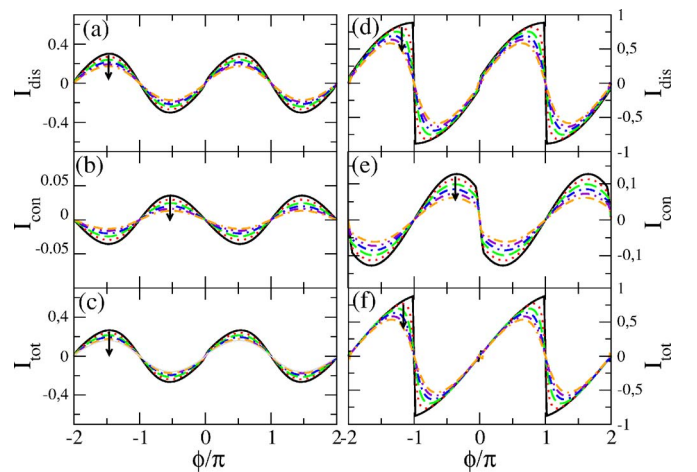


FIG. 3. (Color online) $t/\Gamma \geq 1$. Left (right) panel corresponds to the parallel (serial) case. (a) and (d) discrete I_{dis} , (b) and (e) continuum I_{con} , and (c) and (f) total supercurrent I_{tot} vs ϕ for $t/\Gamma=0, 0.2, 0.4, 0.6, 0.8$, and 1 ($t/\Gamma=0.2, 0.4, 0.6, 0.8$, and 1) and $\Delta=0.17T_K^0$. Currents are in units of $2|e|/\Delta\hbar$. The curves are arranged with increasing t/Γ in the direction of the arrows.

below for the double quantum dot in parallel) are given (hereafter currents are expressed in units of $2|e|\Delta/\hbar$):¹¹

$$I_{\text{dis}} = -2t^2 \sin(2\phi) \sum_{E_p} \frac{s^2(\epsilon)}{\Delta \mathcal{D}'(\epsilon)} \Big|_{\epsilon=E_p}, \quad (17a)$$

$$I_{\text{con}} = -2t^2 \sin(2\phi) \text{Im} \int_{-\infty}^{-\Delta} d\epsilon \frac{1}{\Delta \mathcal{D}(\epsilon)}. \quad (17b)$$

In Eq. (17a) the summation is over all Andreev states $E_p \in [-\Delta, \epsilon_F]$ (ϵ_F is the Fermi energy). Interestingly, we will see below [see Eq. (28)] that in the deep Kondo limit ($\Delta \ll T_K$), we recover the short-junction limit for the Josephson current through a resonant level.^{11,18} In this limit the continuum contribution is almost negligible. For $\Delta \lesssim T_K$ the contributions from the continuum part become considerable.

III. RESULTS

Next we present our results for the double quantum dot in parallel and in a series, respectively. We will choose $\epsilon_0 = -3.25$, $D=100$ (bandwidth), $\epsilon_F=0$, and different values for the rest of the parameters at zero temperature. For these values $T_K^0 = D \exp(-\pi|\epsilon_0|/\Gamma) \approx 0.0036$. All energies are given in units of Γ .

A. Double quantum dot in parallel

The problem is greatly simplified by the transformation

$$c_{k\alpha\sigma} = (c_{k_e\sigma} \pm c_{k_o\sigma})\sqrt{2}, \quad f_{1(2)\sigma} = (f_{e\sigma} \pm f_{o\sigma})\sqrt{2}. \quad (18)$$

The SBMF Hamiltonian is mapped into two independent Josephson junctions (“even” and “odd”) through *effective* resonant levels at $\tilde{\epsilon}_0 \pm \tilde{\tau}$. Each of the two resonant levels accommodates an Andreev state E_{elo} and carries Josephson current

$$I_{\text{tot}}(\phi) = -\frac{2e\Delta}{\hbar} (I_e + I_o). \quad (19)$$

For the double quantum dot in parallel, the Andreev bound states (E_{elo}) and Josephson current are conveniently expressed in the even/odd basis. The Andreev bound states are given as the solutions of

$$\begin{aligned} \mathcal{D}_{elo}(\epsilon) = & \epsilon^2 (\sqrt{\Delta^2 - \epsilon^2} + \tilde{\Gamma})^2 - (\tilde{\epsilon}_0 \pm \tilde{\tau})^2 (\Delta^2 - \epsilon^2) \\ & - \Delta^2 \Gamma^2 \cos^2(\phi). \end{aligned} \quad (20)$$

The discrete and continuum parts of the current are, respectively, given by

$$I_{\text{dis}}^{elo} = -\frac{\sin(2\phi) s^2(\epsilon)}{\Delta \mathcal{D}'_{elo}(\epsilon)} \Big|_{\epsilon=E_{elo}} \quad (21)$$

and

$$I_{\text{con}}^{elo} = -\sin(2\phi) \int_{-\infty}^{-\Delta} d\epsilon s^2(\epsilon) \text{Im} \left[\frac{1}{\Delta \mathcal{D}_{elo}(\epsilon)} \right]. \quad (22)$$

Typical profiles of Andreev states on double quantum dot in parallel are shown in the left panels of Fig. 1. Josephson

currents are shown in the left panels of Fig. 2 ($t \leq \Gamma$) and Fig. 3 ($t \geq \Gamma$). We note that in the deep Kondo limit $\Delta \ll T_K$ the double quantum dot in parallel presents short-junction limit behavior.^{11,18} The Andreev states and the Josephson currents are given by the corresponding expressions

$$E_{elo} = \Delta [1 - \mathcal{T}_{elo} \sin^2(\phi)]^{1/2} \quad (23)$$

and

$$I_{elo}(\phi) = \mathcal{T}_{elo} \sin 2\phi [1 - \mathcal{T}_{elo} \sin^2 \phi]^{-1/2}, \quad (24)$$

with

$$\mathcal{T}_{elo} = 4 \frac{\tilde{\Gamma}^2}{(\tilde{\epsilon}_{elo}^2 + \tilde{\Gamma}^2)}. \quad (25)$$

For very small t/Γ both dots have their own Kondo resonances at ϵ_F and the Josephson current resembles that of a ballistic junction. As t/Γ increases the even and odd Kondo resonances $\tilde{\epsilon}_0 \pm \tilde{\tau}$ move away from ϵ_F and as a result $I_{\text{tot}}(\phi)$ diminishes becoming more sinusoidal

$$I_{elo}(\phi) \approx \mathcal{T}_{elo} \sin 2\phi. \quad (26)$$

The critical current, defined as the maximum supercurrent at phase ϕ_c , is more accessible experimentally.¹⁹ In our case,

$$I_c \approx 2e\Delta/\hbar \sum_{\beta \in \{e,o\}} [1 - (1 - \mathcal{T}_\beta)^{1/2}], \quad (27)$$

and hence decreases with t/Γ . Notice that in spite of the simple formal expression for I_{elo} , the critical current I_c depends on the *many-body* parameters, $\tilde{\Gamma}$ and $\tilde{\epsilon}_0 \pm \tilde{\tau}$, in a non-trivial manner through the solution of Eq. (8).

B. Double quantum dot in a series

A completely different physical scenario is found for the serial configuration. Here the even/odd channels are no longer decoupled and cause novel interference. The manifestation of the interference can be first seen in the profiles of the Andreev states as depicted in Fig. 1. An important difference from the parallel case is the almost flat spectrum with values close to $E_{elo}(\phi) \lesssim \Delta$ (reflecting a very small supercurrent as seen below). As t/Γ increases the spectrum possesses larger amplitude, and for $t/\Gamma \approx 1$ we eventually recover the spectrum of a ballistic junction $E_{elo}(\phi) \approx \Delta \cos(\phi)$. For $t/\Gamma \geq 1$ gaps are opened again [suggesting that $I_{\text{tot}}(\phi)$ diminishes, see below].

Formally, the supercurrent, for $\Delta \ll T_K$, is still given by the expression

$$I(\phi) = \mathcal{T} \sin 2\phi [1 - \mathcal{T} \sin^2 \phi]^{-1/2}, \quad (28)$$

but now the transmission \mathcal{T} is

$$\mathcal{T} = \frac{4\tilde{\tau}^2 \tilde{\Gamma}^2}{\{[(\tilde{\epsilon}_0 - \tilde{\tau})^2 + \tilde{\Gamma}^2][(\tilde{\epsilon}_0 + \tilde{\tau})^2 + \tilde{\Gamma}^2]\}}. \quad (29)$$

We can interpret that for small t/Γ the Cooper pairs hop directly between the two Kondo resonances and $\mathcal{T} \propto (t/\Gamma)^2$.

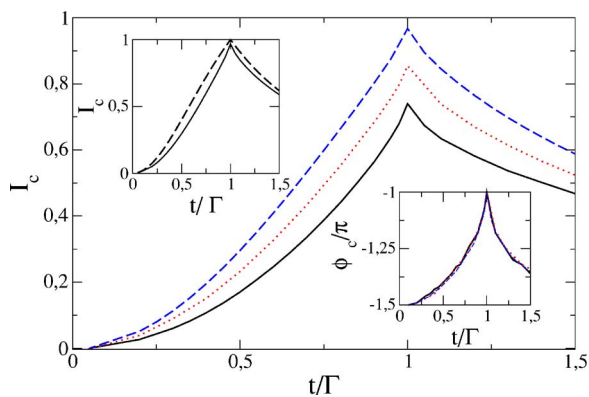


FIG. 4. (Color online) Critical current as a function of t/Γ for $\Delta/T_K^0=0.1, 0.25$, and 0.5 (top to bottom). Upper left inset: comparison with the Josephson critical current given by Eq. (28) (dashed line) for $\Delta/T_K^0=0.1$. Lower right inset: critical phase at which the maximum current occurs.

The supercurrent presents a sinusoidal-like behavior as shown in Fig. 2. With t/Γ increasing, the physical situation changes drastically around $t/\Gamma=1$, where the Kondo singularities of each dot hybridize into a correlated state as a result of the coherent superposition of both Kondo states. We find $\mathcal{T}\approx 1$ and consequently the supercurrent-phase relation exhibits a typical ballistic-junction behavior (see Fig. 3). Further increasing t/Γ makes $I_{\text{tot}}(\phi)$ smaller, which is attributed to the formation of bonding and antibonding Kondo resonances. This results in a nonmonotonous behavior of I_c as a function of t/Γ (shown in Fig. 4 for $\Delta/T_K^0=0.1, 0.25$, and 0.5 , from top to bottom), with a maximum at $t=\Gamma$ (coherent superposition of both Kondo resonances). For the lowest gap (in the short junction regime) the maximum critical current reaches the universal value of $2e\Delta/h$ as expected.¹⁸

The physics of the tunability of I_c as a function of t/Γ is similar to the transistorlike control of supercurrents in a carbon nanotube quantum dot connected to superconducting reservoirs recently reported by Jarillo *et al.*¹⁹ These experiments demonstrate that the supercurrent flowing through the quantum dot can be varied by means of a gate voltage which tunes on- and off-resonance successive discrete levels of the

quantum dot with respect to ϵ_F of the reservoirs. In our case, the Kondo resonances play the role of the discrete levels in the experiments of Ref. 19 whereas t/Γ is the extra knob that tunes the position of the Kondo resonances and thus modulates the critical current. Interestingly, in our case, (i) the supercurrent is mediated by a coherent many-body state (the Kondo resonance) instead of a single particle one and (ii) the maximum supercurrent at $t=\Gamma$ corresponds to coherent transport of Cooper pairs through the whole device whereas an increase of $t/\Gamma\geq 1$ splits the Kondo resonance into two (bonding and antibonding) resulting in a splitting of the Cooper pair into two electrons (one on each resonance) and thus a reduction of the supercurrent. This suggests the use of the Kondo effect as an alternative to previous proposals using double quantum dots¹² for generating and manipulating entangled pairs in a controlled way.

For the experimental realization of the superconducting Kondo double quantum dot, we propose carbon nanotubes since (i) they show Kondo physics,²⁰ (ii) it is possible to fabricate tunable double quantum dots,²¹ and (iii) they are ideal systems to attach new material as electrodes.⁶

IV. CONCLUSIONS

We have studied Cooper pair transport through an artificial Kondo molecule. We find remarkable differences in the phase-current relation between serial and parallel configurations of the double quantum dot. For a double quantum dot in parallel, the supercurrent always decreases with t/Γ whereas for a serial configuration the current behaves nonmonotonously. This fact allows an extra control of the critical current, and thus of Cooper pairs, through Kondo molecules by simply tuning the interdot tunneling coupling.

ACKNOWLEDGMENTS

We acknowledge D. Sánchez for fruitful and long discussions. Work supported by the Spanish MEC through Grant No. MAT2005-07369-C03-03 and the Ramon y Cajal program (R.L.), the SRC/ERC program (R11-2000-071), the KRF Grant (KRF-2005-070-C00055), the SK Fund, and the KIAS.

¹A. C. Hewson, *The Kondo Problem to Heavy Fermions* (Cambridge University Press, Cambridge, England, 1993).

²L. I. Glazman and M. E. Raikh, *Pis'ma Zh. Eksp. Teor. Fiz.* **47**, 378 (1988) [*JETP Lett.* **47**, 452 (1988)]; T. K. Ng and P. A. Lee, *Phys. Rev. Lett.* **61**, 1768 (1988).

³W. G. van der Wiel, S. De Franceschi, T. Fujisawa, J. M. Elzerman, S. Tarucha, and L. P. Kouwenhoven, *Science* **289**, 2105 (2000).

⁴D. Goldhaber-Gordon, H. Shtrikman, D. Mahalu, D. Abusch-Magder, U. Meirav, and M. A. Kastner, *Nature (London)* **391**, 156 (1998); S. M. Cronenwett, T. H. Oosterkamp, and L. P. Kouwenhoven, *Science* **281**, 540 (1998); J. Schmid, J. Weis, K. Eberl, and K. v. Klitzing, *Physica B* **256–258**, 182 (1998).

⁵L. P. Kouwenhoven and L. Glazman *Phys. World* **14**, 33 (2001).

⁶M. R. Buitelaar, T. Nussbaumer, and C. Schönberger, *Phys. Rev. Lett.* **89**, 256801 (2002); M. R. Buitelaar, W. Belzig, T. Nussbaumer, and B. Babic, C. Brader, and C. Schönberger, *ibid.* **91**, 057005 (2003).

⁷A. F. Andreev, *Zh. Eksp. Teor. Fiz.* **46**, 1823 (1964) [*Sov. Phys. JETP* **19**, 1228 (1964)]; *Zh. Eksp. Teor. Fiz.* **49**, 655 (1966) [*Sov. Phys. JETP* **22**, 455 (1966)].

⁸B. J. van Wees and H. Takayanagi, in *Mesoscopic Electron Transport*, edited by L. L. Schön *et al.* (Kluwer, Dordrecht, 1997).

⁹G. Sellier, T. Kopp, J. Kroha, and Yu. S. Barash, *Phys. Rev. B* **72**, 174502 (2005); M.-S. Choi, M. Lee, K. Kang, and W. Belzig, *ibid.* **70**, 020502(R) (2004); *Phys. Rev. Lett.* **94**, 229701 (2005);

- F. Siano and R. Egger, *ibid.* **93**, 047002 (2004); **94**, 229702 (2005); E. Vecino, A. Martín-Rodero, and A. L. Yeyati, Phys. Rev. B **68**, 035105 (2003); A. L. Yeyati, A. Martín-Rodero, and E. Vecino, Phys. Rev. Lett. **91**, 266802 (2003); Y. Avishai, A. Golub, and A. D. Zaikin, Phys. Rev. B **67**, 041301(R) (2003); A. V. Rozhkov and D. P. Arovas, *ibid.* **62**, 6687 (2000); A. V. Rozhkov, D. P. Arovas, and F. Guinea, *ibid.* **64**, 233301 (2001); A. A. Clerk and V. Ambegaokar, *ibid.* **61**, 9109 (2000).
- ¹⁰I. O. Kulik, Zh. Eksp. Teor. Fiz. **49**, 585 (2000) [Sov. Phys. JETP **22**, 841 (1966)]; H. Shiba and T. Soda, Prog. Theor. Phys. **41**, 25 (1969); B. I. Spivak and S. A. Kivelson, Phys. Rev. B **43**, 3740 (1991).
- ¹¹L. I. Glazman and K. A. Matveev, Pis'ma Zh. Eksp. Teor. Fiz. **49**, 570 (1989) [JETP Lett. **49**, 659 (1989)].
- ¹²M. S. Choi, C. Bruder, and D. Loss, Phys. Rev. B **62**, 13569 (2000).
- ¹³P. Coleman, Phys. Rev. B **29**, 3035 (1984); For a review, see D. M. Newns and N. Read, Adv. Phys. **36**, 799 (1987).
- ¹⁴A. Georges and Y. Meir, Phys. Rev. Lett. **82**, 3508 (1999); R. Aguado and D. C. Langreth, *ibid.* **85**, 1946 (2000); Phys. Rev. B **67**, 245307 (2003); T. Aono and M. Eto, *ibid.* **63**, 125327 (2001); R. López, R. Aguado, and G. Platero, Phys. Rev. Lett. **89**, 136802 (2002); P. Simon, R. López, and Y. Oreg, *ibid.* **94**, 086602 (2005).
- ¹⁵Using the EOM technique the off-diagonal matrix GFs are $\hat{G}_{i,k\alpha\sigma} = \tilde{V}_i g_{k\alpha} \hat{\sigma}_z \hat{G}_{i\sigma}$ where $g_{k\alpha}$ is the noninteracting matrix GF for the BCS superconducting leads. The off-diagonal dot matrix GF is $\hat{G}_{i,j\sigma} = \sum_{q\beta} \hat{g}_{j\sigma} \tilde{V}_j \sigma_z \hat{G}_{j,q\beta\sigma} + \hat{g}_{j\sigma} \tilde{\sigma}_z \hat{G}_{i\sigma}$. (To simplify the notation we have omitted the integration along the complex time contour in the previous expressions.)
- ¹⁶R. López, R. Aguado, and G. Platero, Phys. Rev. B **69**, 235305 (2004).
- ¹⁷For a double quantum dot connected in series to normal metallic leads, T_K has an exponential dependence on t ; $T_K \approx T_K^0 e^{t/\Gamma \tan^{-1}(t/\Gamma)}$.
- ¹⁸C. W. J. Beenakker and H. Van Houten, *Single-Electron Tunneling and Mesoscopic Devices*, edited by H. Koch, and H. Lbbig (Springer, Berlin, 1992).
- ¹⁹P. Jarillo-Herrero, J. A. van Dam, and L. P. Kouwenhoven, Nature (London) **439**, 953 (2006).
- ²⁰J. Nygård, D. H. Cobden, and P. E. Lindelof, Nature (London) **408**, 342 (2000).
- ²¹N. Mason, M. J. Biercuk, and C. M. Marcus, Science **303**, 655 (2004); S. Sapmaz, C. Meyer, P. Beliczynski, P. Jarillo-Herrero, and L. P. Kouwenhoven, Nano Lett. **6**, 1350 (2006); M. R. Graber, W. A. Coish, C. Hoffmann, M. Weiss, J. Furer, S. Oberholzer, D. Loss, and C. Schönenberger Phys. Rev. B **74**, 075427 (2006).